Extension of the Sweet-Parker Magnetic Reconnection to the Relativistic Plasma

Hiroyuki R. Takahashi, Tomoyuki Hanawa[1)] and Ryoji Matsumoto[2)]

Graduate School of Science and Technology, Chiba University, Chiba 263-8522, Japan
[1)] *Centre for Frontier Science, Chiba University, Chiba 263-8522, Japan*
[2)] *Deartment of Physics, Graduate School of Science, Chiba University, Chiba 263-8522, Japan*

(Received: 1 September 2008 / Accepted: 28 January 2009)

We study the magnetic reconnection for relativistic plasma in the framework of magnetohydrodynamics and by means of the Particle-In-Cell (PIC) simulation. In the former approach, the magnetic fields are assumed to reconnect steadily inside the diffusion region as assumed in the conventional Sweet-Parker model. The model takes account of the pressure gradient between the diffusion and outflow regions as well as increase in the inertia due to the thermal energy. At a given inflow velocity (reconnection rate), the outflow velocity is faster when the Poynting to plasma kinetic fluxes in the inflow region (namely the magnetization parameter $\sigma_{\rm i}$) is larger. For $\sigma_{\rm i} \gg 1$, the plasma outflow velocity decreases with the increase in the inflow velocity since the larger heating rate enhances the inertia.

We also carried out 2-dimensional PIC simulations to study the $\sigma_{\rm i}$-dependence of the outflow speed. The results indicate that the outflow velocity converges to a saturation value in the limit of large $\sigma_{\rm i}$. On the other hand, the thermal energy increases with $\sigma_{\rm i}$ without saturation. These results are consistent with those based on the MHD analysis.

Keywords: relativistic plasma, magnetic reconnection, magnetohydrodynamics (MHD), Particle-In-Cell simulation

1. Introduction

Magnetic reconnection is an important energy conversion process in astrophysical plasma. The magnetic energy liberated by changing the magnetic field topology heats and accelerates the plasma. In the non-relativistic magnetic reconnection, the outflow from the diffusion region is accelerated up to the Alfvén velocity in the inflow region (e.g., [1]). In the relativistic plasma in which the magnetic energy density exceeds the rest mass energy density, the outflow speed from the reconnection region approaches the light speed.

The magnetic reconnection can power astronomical phenomena such as the pulsar winds [2, 3], soft gamma-ray repeaters [4, 5], and gamma ray bursts [6, 7]. Magnetic reconnection also takes place in relativistic jets observed in active galactic nuclei (AGNs) such as radio galaxies and quasars, and galactic microquasars.

Blackman & Field [8] and Lyutikov & Uzdensky [9] studied the relativistic Sweet-Parker magnetic reconnection model. They concluded that the reconnection rate is enhanced due to the Lorentz contraction. The speed of the outflow from the magnetic reconnection is proportional to the magnetization parameter of the inflow. They assumed that all the magnetic energy flowing to the diffusion region is converted to the kinetic energy; they ignored the gas pressure in the outflow region. Lyubarsky [10] pointed out the importance of the increase in the inertia due to the large thermal energy in the diffusion region. In relativistic plasma, the thermal energy contributes to the inertia especially when it exceeds that of the rest mass. He concluded that the outflow speed from the diffusion region is non-relativistic or semi-relativistic at most. He also concluded that the reconnection rate is not enhanced in contrast to the previous suggestions [8, 9]. However he did not take account of the possibility that the enthalpy and the inertia may be lower in the outflow region than at the neutral point.

Recently, Takahashi et al. [11] obtained the outflow speed from the relativistic magnetic reconnection by taking into account the pressure gradient. In the following, after summarizing the results by Takahashi et al. [11], we compare the results with those obtained by Particle-In-Cell (PIC) simulations.

2. MHD Theory of Relativistic Reconnection

We consider a 2-dimensional steady state reconnection in $X - Y$ plane. The electric resistivity is assumed to be appreciable only within the diffusion region, $|X| \leq L$ and $|Y| \leq \delta$ (see, Fig. 1). Thus the ideal MHD condition is applied outside the diffusion region. We assume $B_{\rm z} = 0$ (without guide field). The proper density ρ, proper gas pressure p, magnetic field $\boldsymbol{B}$, bulk flow velocity $\boldsymbol{v} = c\boldsymbol{\beta}$ are assumed to be constant in the inflow and outflow regions. All the variables with the subscript i denote the values in the inflow region, while those with the subscript o do the

author's e-mail: takahasi@astro.s.chiba-u.ac.jp

©2009 by The Japan Society of Plasma Science and Nuclear Fusion Research

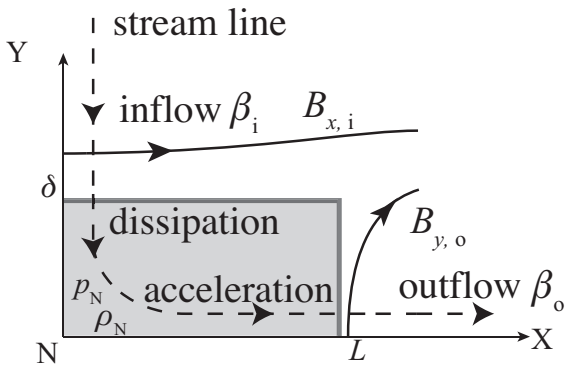

Fig. 1 Schematic picture of the Sweet-Parker magnetic reconnection in $X-Y$ plane. Only the first quadrant is shown. The electric resistivity is non-zero in the shaded region. Solid curves depict magnetic field lines. A stream line is shown by the dashed curve.

values in the outflow region.

From the mass and energy conservation equations, we obtain

$$\rho_{\rm i}\gamma_{\rm i}\beta_{\rm i}L = \rho_{\rm o}\gamma_{\rm o}\beta_{\rm o}\delta, \tag{1}$$

$$\rho_{\rm i}c^2\gamma_{\rm i}^2\beta_{\rm i}L\,(1+\sigma_{\rm i}) = \rho_{\rm o}c^2\gamma_{\rm o}^2\beta_{\rm o}\delta\,(1+\alpha_{\rm o}+\sigma_{\rm o})\,, \tag{2}$$

where

$$\alpha \equiv \frac{\Gamma}{\Gamma-1}\frac{p}{\rho c^2}, \tag{3}$$

and

$$\sigma \equiv \frac{|\boldsymbol{B}|^2}{4\pi\rho c^2\gamma^2}. \tag{4}$$

Here we assume that the thermal pressure is small and can be ignored in the inflow region. The symbol α denotes the ratio of thermal enthalpy and the rest mass energy. The specific heat ratio Γ is taken to be 4/3. The symbol σ denotes the magnetization parameter. We obtain

$$\beta_{\rm i}B_{x,{\rm i}} = \beta_{\rm o}B_{y,{\rm o}}. \tag{5}$$

from the X- and Y-component of the induction equation.

From equations (1) and (2), we obtain

$$(1+\sigma_{\rm i})\,\gamma_{\rm i} = (1+\alpha_{\rm o}+\sigma_{\rm o})\,\gamma_{\rm o}. \tag{6}$$

This equation is equivalent to the Bernoulli's theorem and means that the specific enthalpy remains constant. The enthalpy is the product of the Lorentz factor and the inertia. The inertia includes thermal and magnetic energies as well as the rest mass, since we are dealing with relativistic plasma. To produce an ultra-relativistic outflow ($\gamma_{\rm o} \gg 1$), the inertia in the outflow region should be much smaller than the specific enthalpy of the inflow.

When the inflow ($\beta_{\rm i}$, $B_{x,{\rm i}}$, $\rho_{\rm i}$) and the size of the diffusion region (L and δ) are given, equations (1), (5), and (6) give us three independent relations for four unknowns, $\beta_{\rm o}$, $B_{x,{\rm o}}$, $\rho_{\rm o}$, and $p_{\rm o}$. An independent relation is required to determine the outflow. A simple solution to close the equations is to ignore the thermal pressure in the outflow region by assuming $p_{\rm o} = 0$ [8, 9]. Lyubarsky [10] pointed out the importance of the increase in the inertia due to the enhanced thermal energy and solved the momentum equation between the neutral point and the outflow region. He evaluated the thermal enthalpy of the plasma in the acceleration region by using the gas pressure at the neutral point $p_{\rm N}$. Here we take into account the pressure gradient between the neutral point and the outflow region, which accelerates the outflowing plasma.

Suppose that the plasma is heated by dissipation of magnetic energy near the neutral point. The pressure balance across the current sheet implies

$$p_{\rm N} = \frac{B_{x,{\rm i}}^2}{8\pi}, \tag{7}$$

We assume that the density of the plasma in the neutral sheet is the same as that of the inflow,

$$\rho_{\rm N} = \rho_{\rm i}, \tag{8}$$

where $\rho_{\rm N}$ is the plasma density at the neutral point. In other words, the magnetic energy release is so prompt that the plasma does not have time to expand in the neutral sheet. We assume that the plasma evolves adiabatically after the prompt heating by magnetic energy release. We then obtain the closure relation,

$$\frac{p_{\rm N}}{\rho_{\rm N}^{\Gamma}} = \frac{p_{\rm o}}{\rho_{\rm o}^{\Gamma}}. \tag{9}$$

The equations (1), (5), (6), (7), (8), and (9) give us the relation between the inflow and outflow.

The specific momentum of the outflow $u_{\rm o} = \gamma_{\rm o}\beta_{\rm o}$ is shown as a function of $\sigma_{\rm i}$ in Fig. 2 for $\beta_{\rm i} = 10^{-5}$. The thick curve denotes the result for $L/\delta = 10$, while the thin curve does for $L/\delta = 100$.

The specific momentum of the outflow increases with $\sigma_{\rm i}$, when $\beta_{\rm i}$ and L/δ are fixed. It is saturated in the limit of large $\sigma_{\rm i}$, while it is proportional to $\sqrt{\sigma_{\rm i}}$ when $\sigma_{\rm i}$ is small.

When the outflow is cold ($\alpha_{\rm o} \ll 1$), the approximate solution can be obtained as

$$\gamma_{\rm o} \simeq (1+\sigma_{\rm i})\gamma_{\rm i}. \tag{10}$$

This relation is equivalent to that by Lyutikov & Uzdensky [9]. When $\sigma_{\rm i} \ll 1$, the outflow velocity is $v_{\rm o} \simeq \sqrt{2}v_{\rm A}$, where $v_{\rm A}$ is the Alfvén velocity in the inflow region. This result is equivalent to that of the conventional Sweet-Parker magnetic reconnection model when $p_{\rm o} = p_{\rm i}$ (see, e.g., [1]).

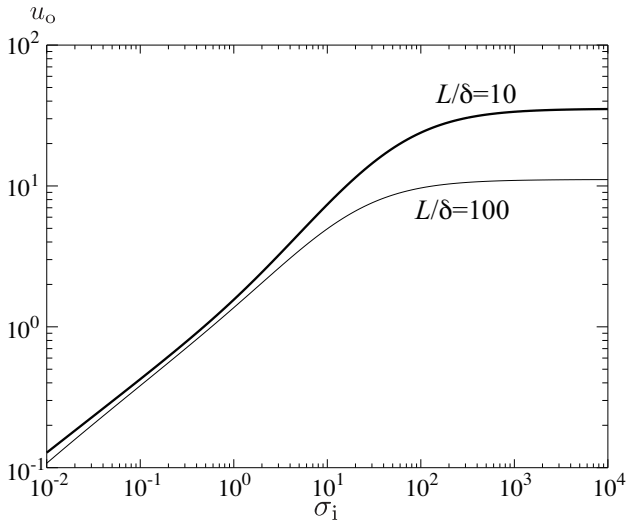

Fig. 2 Specific momentum of the outflow $u_o \equiv \gamma_o\beta_o$ as a function of the magnetization parameter σ_i for $\beta_i = 10^{-5}$. The thick curve denotes u_o for $L/\delta = 10$, while the thin curve does for $L/\delta = 100$.

When the outflow is relativistically hot ($\alpha_o > 1$), the specific momentum of outflow u_o approaches to

$$u_o \sim u_o^{sat} = \sqrt{\frac{1}{8}\frac{\delta}{L}\frac{1}{\beta_i}}. \tag{11}$$

Note that the outflow velocity is reciprocal to square root of the inflow velocity. This indicates that the outflow velocity is slower for a larger reconnection rate. The outflow velocity is smaller than the Alfvén velocity for a relativistically hot plasma because of the large inertia. Note that the heating rate is larger for a larger reconnection rate. A hot relativistic plasma is hard to be accelerated and tends to be jammed in the diffusion region. Hence the outflow is hotter and slower when the reconnection rate is larger.

The outflow velocity is relativistic only when the inflow speed is very low, so that the outflow is cold. Equation (11) gives us the condition for a relativistic outflow,

$$\beta_i \ll \delta/L\,. \tag{12}$$

The maximum inflow velocity is estimated to be $\beta_{i,max} \simeq \delta/L$ from the condition that equation (6) has a solution. When the reconnection rate is high ($\beta_i \simeq \delta/L$), the outflow remains relativistically hot and can be only weakly relativistic as pointed out by Lyubarsky [10] even after the adiabatic expansion. Lyubarsky [10] already pointed out that the pressure should decrease significantly towards the outflow region in order the outflow to be highly relativistic. Such a situation can be realized when the reconnection rate is sufficiently small, $\beta_i \ll \delta/L$.

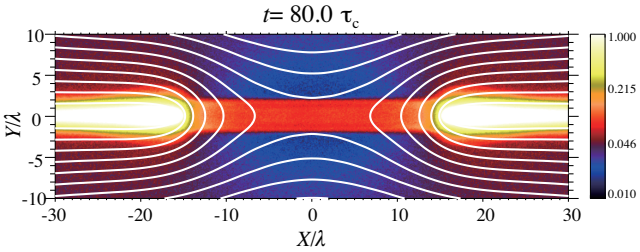

Fig. 3 Plasma density (color) and magnetic field lines (white curves) at $t = 80\tau_c$ for $k_BT_c/mc^2 = 0.1$ corresponding to $\sigma_i = 3.8$.

3. PIC simulation

We carried out 2-dimensional relativistic Particle-In-Cell (PIC) simulations for pair plasma to study the σ_i-dependence of the outflow velocity. The initial condition is given by a relativistic Harris configuration [12]. The number of grid points in the simulation box is $(N_X, N_Y) = (1024, 512)$. We imposed the periodic boundary conditions in both the directions. We employed $\sim 6.7\times10^7$ electron-positron pairs. The length and the time are normalized by the width of the current sheet λ and the light crossing time $\tau_c = \lambda/c$, respectively. We used 10 grid points in λ and the corresponding simulation box size is $-51.2 \le X/\lambda \le 51.2$ and $-38.4 \le Y/\lambda \le 12.8$. Besides the current sheet at $Y = 0$, another current sheet is placed at $Y/\lambda = -25.6$ for the periodic boundary. In other words, the region of $-38.4 \le Y/\lambda \le -12.8$ is a mirror. The drift velocity is fixed at $v_d = 0.3c$ in the current sheet. The temperature of the background plasma (T_i) is 0.2 times lower than that in the current sheet (T_c) and the density of the background plasma (n_i) is 5% of that of the current sheet ($n_c\gamma_d$) for all simulations. Here n is the proper number density and γ_d is the Lorentz factor of the drift velocity v_d.

The pressure balance across the current sheet gives the following equation;

$$\frac{B_i^2}{8\pi} = 2n_c k_B T_c. \tag{13}$$

This equation gives

$$\sigma_i = \frac{B_i^2}{4\pi(2n_i)\gamma_i^2 m_e c^2} \simeq 2\frac{n_c}{n_i}\frac{k_B T_c}{m_e c^2}. \tag{14}$$

Here we used the approximation $\gamma_i \simeq 1$ in the last equation. This enables us to derive σ_i-dependence of the outflow by changing the temperature inside the current sheet. We carried out simulations for $k_BT_c/m_ec^2 = (0.05, 0.1, 0.5, 1.0, 4.0, 8.0, 16.0)$, corresponding to $\sigma_i = (1.9, 3.8, 19, 38, 153, 305, 611)$. These initial conditions are almost the same as those of Zenitani & Hoshino [13].

To trigger the magnetic reconnection, we imposed a weak electric field around $X = Y = 0$ at the initial

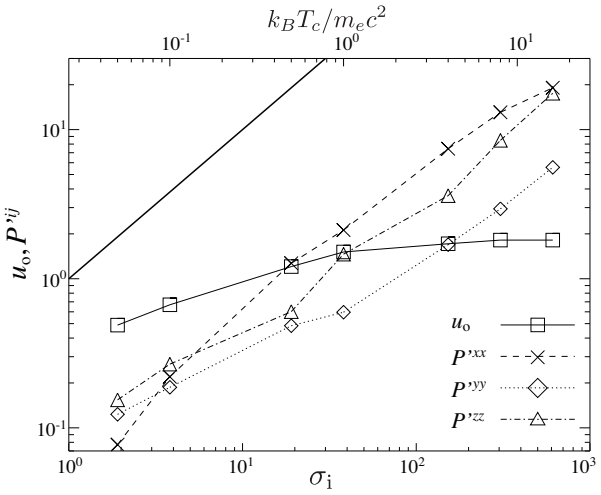

Fig. 4 The maximum outflow four velocity u_o (squares), P'^{xx} (crosses), P'^{yy} (diamonds), P'^{zz} (triangles) inside the diffusion region obtained by PIC simulations are shown as a function of σ_i (lower horizontal axis) and $k_BT_c/(m_ec^2)$ (upper horizontal axis). The energy momentum tensor $P'^{\mu\nu}$ is averaged inside the diffusion region and is normalized by the rest mass energy. Thick solid curve shows $P'^{\mu\nu} \propto \sigma_i$.

state [13]. Particles flowing into the current sheet by the drift motion enter the reconnection region.

After imposing the triggering electric field, magnetic fields are reconnected and plasma flows out to the $\pm$X-direction. Fig. 3 shows the plasma number density (color) and magnetic field lines (white curves) at $t = 80\tau_c$ for $\sigma_i = 3.8$ around the reconnection region. The magnetic field lines in the reconnection region are similar to those of the Sweet-Parker reconnection [13]. The shape of the diffusion region where $(\boldsymbol{E} + \boldsymbol{\beta} \times \boldsymbol{B})_z \neq 0$ is rectangle. No shocks appear in the outflow region. The corresponding Alfvén velocity for $\sigma_i = 3.8$ is $0.87c$, while the maximum outflow velocity is $0.56c$.

Next we evaluate the thermal energy inside the diffusion region. We simply evaluate it from the energy momentum tensor,

$$P^{\mu\nu} = \int \frac{d^3p}{\epsilon}\, p^\mu p^\nu f(t, \boldsymbol{x}, \boldsymbol{p}), \tag{15}$$

where $f(t, \boldsymbol{x}, \boldsymbol{p})$ and ϵ are the particle distribution function and the particle energy, respectively. Since the particles are mainly accelerated in the Z-direction, we need to evaluate the thermal energy by carrying out the Lorentz transformation in the Z-direction as

$$P'^{\mu\nu} = \Lambda^\mu{}_\eta(\beta_z)\Lambda^\nu{}_\rho(\beta_z)P^{\eta\rho}, \tag{16}$$

where Λ is the transformation matrix and β_z is the Z-component of the average velocity inside the diffusion region. We compare them at the moment when the distance between the points of maximum $|B_y(X, Y = 0)|$ reaches 30λ.

Fig. 4 shows the σ_i-dependence of the maximum outflow four velocity u_o (squares), P'^{xx} (crosses), P'^{yy} (diamonds), and P'^{zz} (triangles) for electrons. Here we averaged $P'^{\mu\nu}$ inside the diffusion region and normalized it by the rest mass energy. Other components of the pressure tensor are negligible around the neutral point. The outflow four velocity u_o increases with σ_i for a smaller σ_i, while it is saturated at a certain value in the limit of the large σ_i. When σ_i is large, the outflow velocity is much smaller than the Alfvén velocity of the inflow.

The plasma cannot be accelerated up to the ultra-relativistic speed in spite of the larger free energy (magnetic energy). Fig. 4 shows that the thermal enthalpy increases with σ_i without saturation. It indicates that the magnetic energy is mainly converted to the thermal energy when σ_i is large. These results are consistent with those based on the MHD theory.

In our simulations, the maximum inflow velocity is $0.2 - 0.7c$. It is consistent with those by Zenitani & Hoshino [13]. The aspect ratio of the diffusion region is about 10. These results indicate that the condition given by equation (12) for the relativistic outflow from the magnetic reconnection region is not satisfied. The relativistic outflow is not formed because the larger heating rate results in the larger inertia (enthalpy).

4. Conclusion

We extended the Sweet-Parker model of magnetic reconnection for relativistic plasma. Our model takes into account the pressure gradient between the neutral point and the outflow region. When the inflow velocity is small, the outflow can be ultra-relativistic for a larger σ_i. Meanwhile, when the inflow velocity is large, the outflow velocity cannot exceed the upper limit set by equation (11). The outflow speed is slower for a larger reconnection rate since the larger heating rate results in the increase in the inertia. We also carried out 2-dimensional PIC simulations to study the σ_i-dependence of the outflow velocity. We confirmed that the outflow velocity is saturated at a certain value in the limit of large σ_i, while the thermal enthalpy increases with σ_i monotonically. The outflow velocity is still only mildly relativistic for a larger σ_i. These results are consistent with those obtained from the MHD analysis. The adiabatic expansion is insufficient to accelerate plasma outflow to highly relativistic speed in our PIC simulations.

We are grateful to an anonymous referee for constructive comments improving the paper. The authors thank Hoshino M., Jaroschek C. H. and Zenitani S. for useful discussions. This work is supported by the Grants-in-Aid for Scientific Research of Ministry of Education, Culture, Sports, Science, and Technol-

ogy (TH:19540236, RM:20340040). Numerical computations were carried out on Cray XT4 at Center of Computational Astrophysics, CfCA, of National Astronomical Observatory of Japan.

[1] E. Priest, T. Forbes, *Magnetic Reconnection: MHD Theory and Applications* (Cambridge University Press, Cambridge, 2000)
[2] F. V. Coroniti, ApJ, **349**, 538 (1990).
[3] Y. Lyubarsky, J. G. Kirk, ApJ, **547**, 437 (2001).
[4] C. Thompson, R. C. Duncan, ApJ, **473**, 322 (1996).
[5] M. Lyutikov, MNRAS, **367**, 1594 (2006).
[6] G. Drenkhahn, A&A, **387**, 714 (2002).
[7] G. Drenkhahn, H. C. Spruit, A&A, **391**, 1141 (2002).
[8] E. G. Blackman, G. B. Field, Phys. Rev. Lett., **72**, 494 (1994).
[9] M. Lyutikov, D. Uzdensky, ApJ, **589**, 893 (2003).
[10] Y. E. Lyubarsky, MNRAS, **358**, 113 (2005).
[11] H. R. Takahashi, T. Hanawa, R. Matsumoto, submitted to PASJ (2009).
[12] J. G. Kirk, O. Skæraasen, ApJ, **591**, 366 (2003).
[13] S. Zenitani, M. Hoshino, ApJ, **670**, 702 (2007).